Investigation of the structural, optical and electrical transport properties of n-doped CdSe thin films

Investigation of the structural, optical and electrical transport properties of n-doped CdSe thin films

H M Ali and H A Abd El-Ghanny

Physics Department, Faculty of Science, 82524 Sohag, Sohag University, Egypt

E-mail: hazem95@yahoo.com (H M Ali)

Abstract
Thin films of $(CdSe)_{90}(In_2O_3)_{10}$, $(CdSe)_{90}(SnO_2)_{10}$ and $(CdSe)_{90}(ZnO)_{10}$ have been grown on glass substrates by the electron beam evaporation technique. It has been found that undoped and Sn or In doped CdSe films have two direct transitions corresponding to the energy gaps E_g and $E_g + \Delta$ due to spin–orbit splitting of the valence band. The electrical resistivity for n-doped CdSe thin films as a function of light exposure time has been studied. The influence of doping on the structural, optical and electrical characteristics of In doped CdSe films has been investigated in detail. The lattice parameters, grain size and dislocation were determined from x-ray diffraction patterns. The optical transmittance and band gap of these films were determined using a double beam spectrophotometer. The DC conductivity of the films was measured in vacuum using a two-probe technique.

1. Introduction

Thin films of II–VI semiconductors are of considerable interest due to their excellent optical properties in the visible range. Metal selenide thin films offer a range of optical band gap energies suitable for various optical and optoelectronic applications [1]. These semiconductor materials exist in either zinc-blende (cubic) or wurtzite (hexagonal) modification in the solid state. A cubic modification is expected to be more amenable to doping/alloying than the wurtzite phase so that one can generate semiconductor material with improved properties [2]. Such modifications can be achieved by addition of a suitably chosen third component as an impurity/dopant [3].

Cadmium selenide is one of the promising semiconducting materials that have been studied for application in solar cells, thin film transistors [4–6], gamma-ray detectors [7], photo detection and optoelectronic applications [8]. Major attention has been given in recent years to the investigation of electrical and optical properties of CdSe thin films in order to improve the performances of the devices and also to find new applications. CdSe thin films have been prepared by a number of vacuum and non-vacuum film deposition methods, including vacuum evaporation and coevaporation [9, 10], the electrostatic assisted aerosol jet deposition method [11], laser ablation [12], electrochemical deposition [13], chemical deposition [14], the hot wall deposition technique [15] and spray pyrolysis [16]. The electronic and optical properties of semiconductors are strongly influenced by the methods of preparation, heat treatment, type and level of dopant.

The electron beam evaporation technique offers some major advantages.

(1) It has a high power density, and hence a wide range of control over evaporation rate, from very low to very high.
(2) Because the evaporant is contained in the water-cooled crucible, only its surface gets to a high temperature. Metallurgical reactions between crucible and evaporant leading to film contamination are therefore eliminated.
(3) Electron beam evaporation technique provides economical and efficient usage of evaporant and enables constant rate deposition.

In recent years, we have been engaged in the preparation of transparent conducting film TCOs with a series of oxides [17–24]. In this work, we mainly discuss experimental data for n-doped CdSe thin films. The typical dopants used to obtain n-type CdSe are tin, indium and zinc, as a cation site dopant. Our intention is to employ this material for the fabrication of photovoltaic devices, and therefore as a part of our continuing program we concentrated on our bifocal interest: to investigate and analyze the structural, optical and

electrical transport properties of Sn, In or Zn doped CdSe deposited by the electron beam evaporation technique.

2. Experimental details

The bulk materials of $(CdSe)_{90}In_{10}$, $(CdSe)_{90}Sn_{10}$ and $(CdSe)_{90}Zn_{10}$ were prepared using portions of highly pure (Aldrich, 99.999%) powders of CdSe, Sn, In and Zn. Appropriate ratios of CdSe were thoroughly mixed separately with In, Sn and Zn to form three different compounds. To insure complete mixing, each compound has been ground for at least three hours. Then they have been made into tablets using a cold pressing technique. Sintering (which is often associated with the formation of new bonds, densification and maybe grain growth [19]) of these tablets was carried out at 400 °C for 4 h in air.

Thin films of the prepared $(CdSe)_{90}(In_2O_3)_{10}$, $(CdSe)_{90}$ $(SnO_2)_{10}$ and $(CdSe)_{90}(ZnO)_{10}$ tablets were deposited from a single source at 1×10^{-6} Torr by the electron beam evaporation technique onto ultrasonically cleaned microscope glasses using an Edwards model E306A high vacuum coating unit. This technique involves evaporation of an alloy using a rod-fed electron beam source. Evaporation operates under steady-state conditions, where the composition and volume of the liquid pool on top of a solid rod are kept constant. The deposition rate (4–8 nm min^{-1}) and the film thickness (150 nm) were determined by means of a Maxtek model TM200 digital film thickness monitor.

Investigations of the microstructure were carried out using a Cu Kα x-ray diffractometer (Philips model PW1710, Holland; $\lambda = 1.541\,838$ Å).

A Jasco V-570 UV–visible–NIR spectrophotometer (with photometric accuracy of ± 0.002–0.004 absorbance and $\pm 0.3\%$ transmittance) was employed to record the transmission and reflection spectra over the wavelength range 200–2500 nm at normal incidence.

The electrical resistivity of n-doped CdSe films was measured at room temperature as a function of light exposure time using a Keithley 614 electrometer with simple two-probe contacts. Silver paste electrodes with separation of 2 mm were used. To study the electrical characterization of In doped CdSe films, resistivity measurements were carried out using the two d.c. probe method in the temperature range of 73–525 K. A brass block was used as a sample holder-cum-heater. The areas of the films were defined and silver paste was applied to ensure good electrical contact to the films. A chromel–alumel thermocouple was used for measuring the temperature.

3. Discussion

Figure 1 shows the optical transmittance and reflectance spectra of undoped and n-doped CdSe thin films prepared at room temperature. The optical transmission of undoped CdSe film is above 85% at wavelengths close to 1250 nm and above 60% at the wavelength 750 nm. For Zn doped CdSe, Sn doped CdSe and In doped CdSe, the transmittance values are equal to 66.4%, 60% and 77.3% in the visible region (820, 820 and 750 nm respectively) and 88.2%, 87.8% and 88.5% at
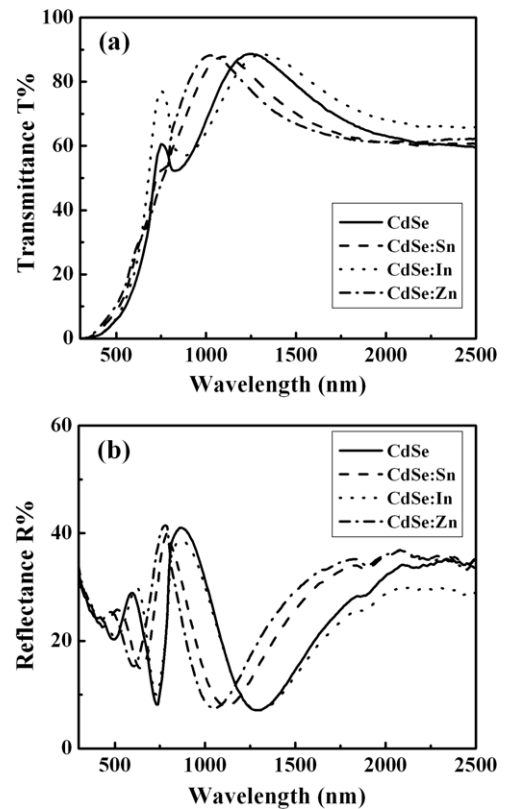

Figure 1. The optical transmittance (a) and reflectance (b) spectra of undoped and n-doped CdSe thin films prepared at room temperature.

the wavelengths 1030, 1095 and 1300 nm respectively. This feature illustrates the good quality of n-doped CdSe thin film deposition by the electron beam evaporation technique.

Several experimental methods enabling an estimate of the energy gap value for these materials have been developed. The most common methods are based on the optical absorption measurements. The estimate of the energy gap value obtained by means of absorption measurements is known as the 'optical gap' [12]. One of the standard empirical methods to obtain the optical gap value is the Tauc method [25]; the optical gap value in the strong absorption region ($\alpha > 10^4$ cm^{-1}) is defined according to the following equation (1):

$$(\alpha h\nu)^2 = A(h\nu - E_g) \qquad (1)$$

where α represents the optical absorption coefficient, h is the Planck's constant, E_g is the energy band gap and A is a characteristic parameter independent of photon energy. The allowed direct band gap E_g values were obtained by extrapolating the linear portion of the plots of $(\alpha h\nu)^2$ versus $h\nu$ to $\alpha = 0$ in the wavelength range from 350 to 850 nm [26]. The plots of $(\alpha h\nu)^2$ versus $h\nu$ for undoped and n-doped cadmium selenide thin films prepared at room temperature are shown in figure 2. It has been found that undoped and Sn or In doped CdSe films have two direct transitions corresponding to the energy gaps E_g and $E_g + \Delta$, where Δ is the spin–orbit splitting. Two regions of $(\alpha h\nu)^2$ versus $h\nu$ for undoped CdSe are plotted separately and shown in figure 3(a). It is clear that there are two exponential regions corresponding to
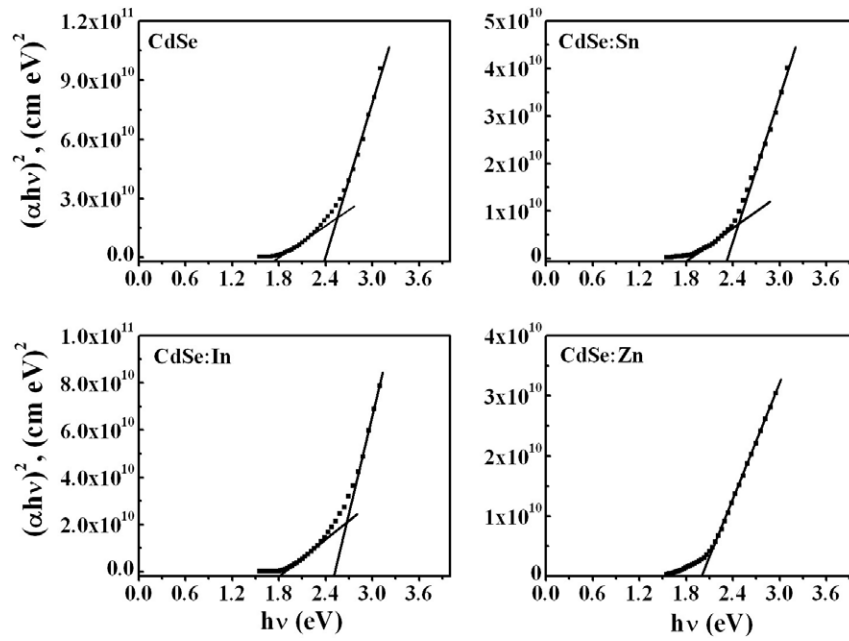
Figure 2. Plot of $(\alpha h\nu)^2$ versus $h\nu$ for undoped and n-doped CdSe thin films prepared at room temperature.
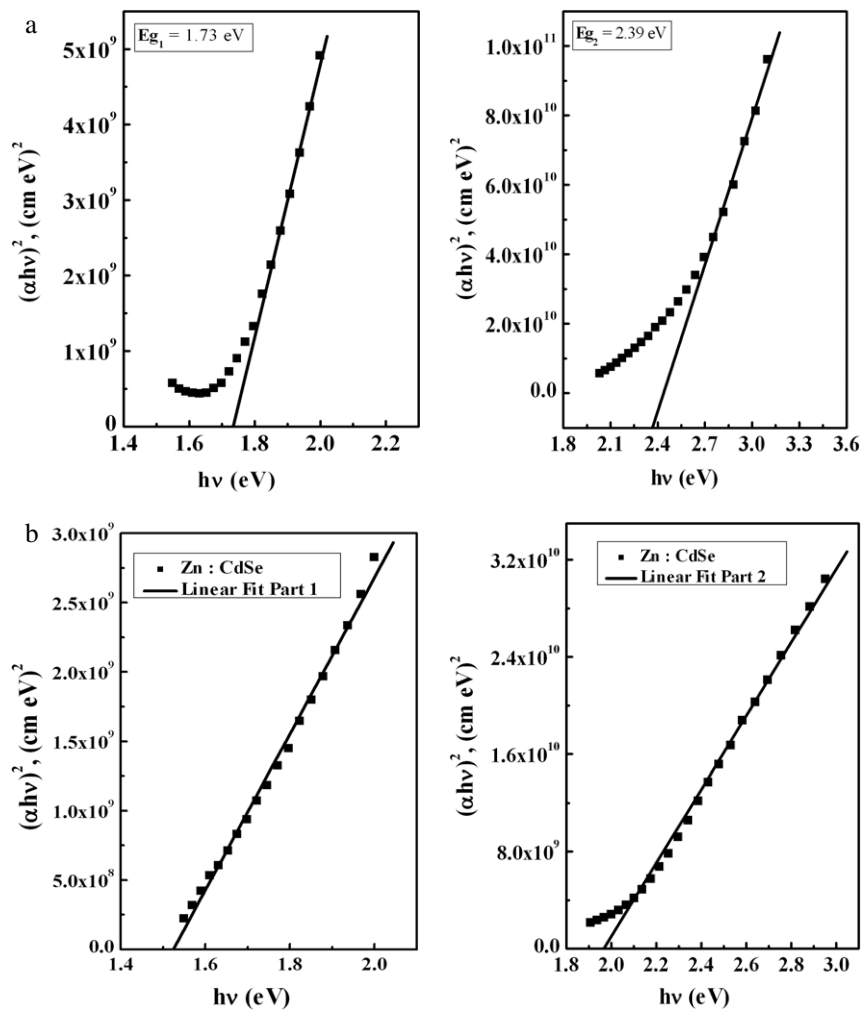

Figure 3. (a) Plots of $(\alpha h\nu)^2$ versus $h\nu$ for undoped CdSe thin films as two exponential regions. (b) Plots of $(\alpha h\nu)^2$ versus $h\nu$ for Zn doped CdSe thin films as two regions.
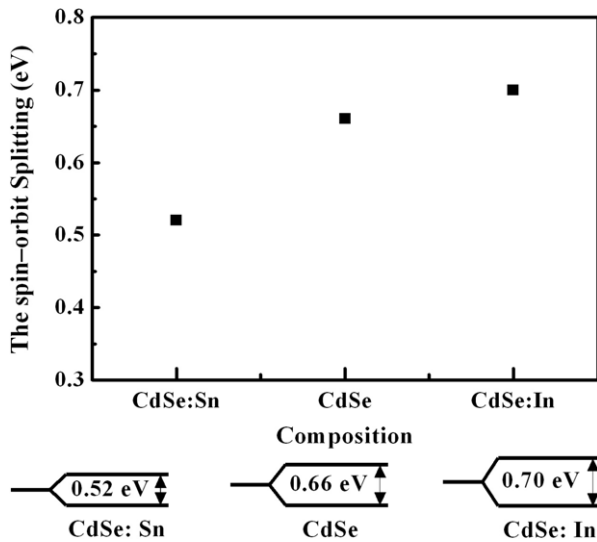
Figure 4. The spin–orbit splitting of the valence band for undoped and n-type doped CdSe thin films.

two different energy gaps. For Sn and In doped CdSe, the same results have been obtained. Similarly, two different band gap energies have been reported by Velumani $et~al$ [27] and Padiyan $et~al$ [1] for CdSe thin films prepared by the thermal evaporation technique. Two different E_g values are expected, if additional absorption processes cause the tail at the absorption edge, because of transitions from the higher valence level. A similar effect should occur for a transition from the lower of the split valence levels [1].

The band gap energies obtained for the undoped film are 1.73 and 2.39 eV. The first energy band gap is very close to its value for bulk material (E_g = 1.75 eV). It is observed that the second energy band gap of undoped CdSe possesses a relatively high value for an unknown reason. For Sn doped CdSe the band gap energies are 1.8 and 2.32 eV, for In doped CdSe they are 1.81 and 2.51 eV and for Zn doped CdSe the band gap energy is equal to 1.98 eV. The two direct transitions can be attributed to spin–orbit splitting of the valence band [28]. These splittings are also noticed in the transmittance spectra of CdSe thin films at 750 nm ($h\nu$ = 1.65 eV) and 1250 nm ($h\nu$ = 0.99 eV) for undoped film and at 750 nm ($h\nu$ = 1.65 eV) and 1095 nm ($h\nu$ = 1.13 eV) for Sn doped CdSe, whereas for In doped CdSe they are at 750 nm ($h\nu$ = 1.65 eV) and 1300 nm ($h\nu$ = 0.95 eV). But no such splitting could be detected for Zn doped CdSe film. Two regions of $(\alpha h\nu)^2$ versus $h\nu$ for Zn doped CdSe are plotted separately, as shown in figure 3(b). It is clear that there is only one exponential region (part 2), whereas the other region (part 1) exhibits a non-exponential part. This indicates that Zn doped CdSe has a unique energy band gap.

Values of the spin–orbit splitting of the valence band for undoped and n-type doped CdSe thin film samples were calculated (by taking the difference between E_{g1} and E_{g2}) and plotted in figure 4.

Figure 5 presents the variations of electrical resistivity for undoped and n-doped CdSe thin films as a function of light exposure time. It is obvious that the electrical resistivity
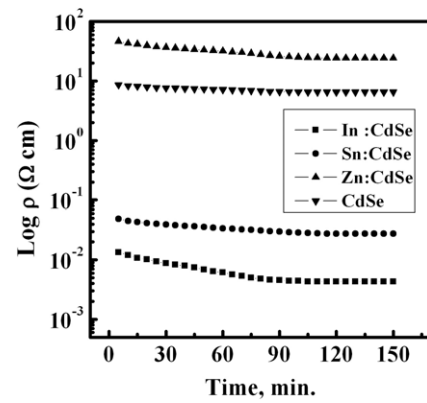

Figure 5. Variations of the electrical resistivity of n-doped CdSe thin films as a function of light exposure time.
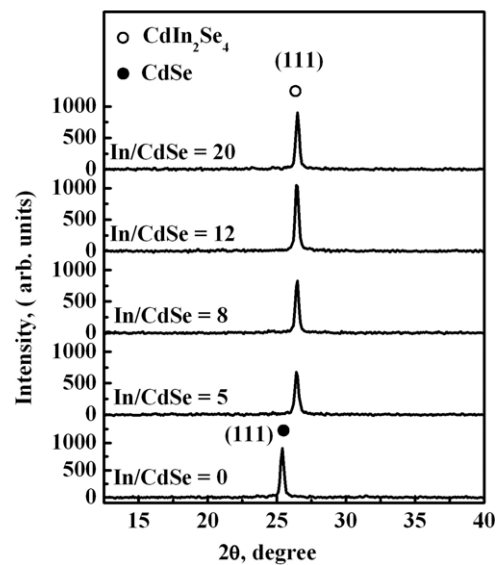

Figure 6. X-ray diffraction pattern of undoped and In doped CdSe thin films.

decreases with increasing light exposure time and the In doped CdSe thin film has the lowest value of resistivity. The decrease of the electrical resistivity with increasing the light exposure time can be attributed to the increase of the mobility carriers.

From the previous results, it is quite clear that In doped CdSe thin film has the best properties in comparison with undoped CdSe, Sn doped CdSe or Zn doped CdSe. So the optical and electrical properties of In doped thin films will be studied in detail as follows.

The x-ray diffraction pattern (figure 6) reveals the existence of a CdSe (111) diffraction peak at d = 3.51 Å (25.35°) for undoped CdSe film and CdSe$_2$In$_4$(111) peak at d = 3.37 Å (26.44°) for In doped CdSe. For In doped CdSe it is evident that there is no CdSe diffraction peak, indicating that the ratio of CdSe and In cations becomes important for obtaining a homogeneous film without secondary phases such as CdSe or In$_2$O$_3$. It is also shown that the intensity of the CdSe$_2$In$_4$ (111) diffraction peak of the growing film increases with further increase in indium content to In = 12 wt%. Besides, for heavily In doped CdSe, the intensity of the
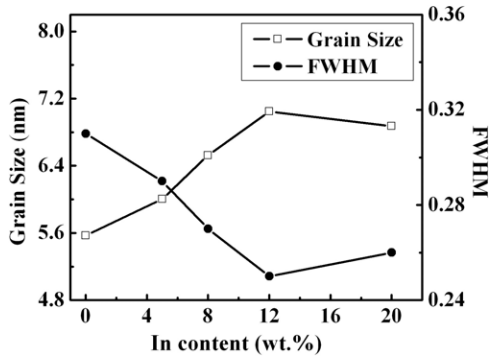
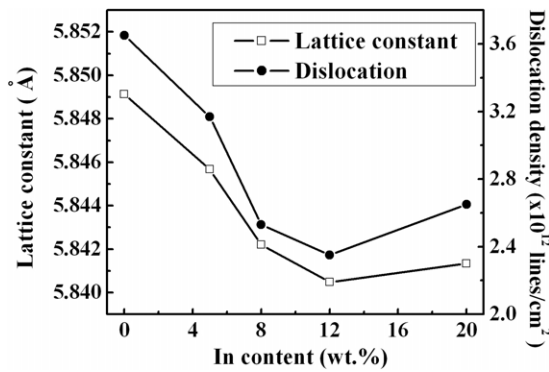**Figure 7.** Variations of FWHM and grain size with In content (wt%).

Figure 8. Variations of the lattice constant and dislocation density with In content (wt%).

Figure 9. The wavelength dependence of optical transmittance of In doped CdSe films.
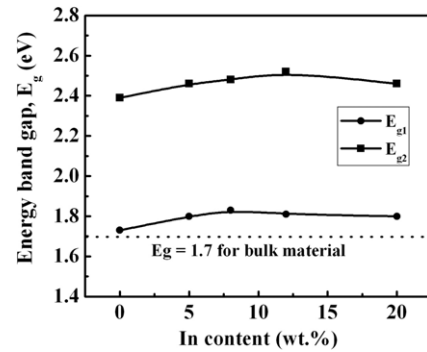
Figure 10. Plot of two distinct values of the optical band gap as a function of In content (wt%).

CdSe$_2$In$_4$ peak decreases, indicating that the local ordering is changed with increasing indium content.

In order to study the effect of doping on the structural characteristics of CdSe films, the lattice constant (a) and the grain size (D) were calculated from the XRD spectra. The lattice constant was calculated using the following equation [29]:

$$d_{(hkl)} = \frac{a}{\sqrt{h^2 + k^2 + l^2}}. \qquad (2)$$

Using the average full width at half maximum (FWHM) of the preferred line, the grain size, D, has been calculated according to the Debye–Scherrer formula as follows [30]:

$$D = \frac{0.9\lambda}{B \cos\theta_{\mathrm{B}}}. \qquad (3)$$

Here, $\lambda = 1.541\,838$ Å and B is the measured broadening of the diffraction line peak at an angle of 2θ at half its maximum intensity (FWHM) in radians. The resulting FWHM and grain size are shown in figure 7 as a function of In content. One can see that the grain size increased with increasing In content up to In = 12 wt%. For heavily doped CdSe at In = 20 wt% the grain size relatively decreased. This behavior of the grain size is related to the film crystallinity. Figure 8 shows the variations of the lattice constant and dislocation density with In content. It is observed that the lattice constant decreases
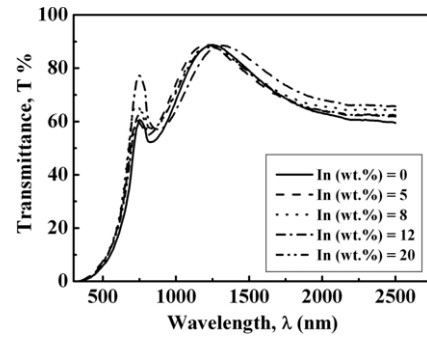
with increasing In content, which can be attributed to the lattice strain [31]. The dislocation density (φ) was evaluated using the formula suggested by Williamson and Smallman [32], which is $\varphi = n/D^2$, where n is a factor that equals unity, giving minimum dislocation density.

$$\text{i.e. } \varphi = 1/D^2. \qquad (4)$$

As shown in figure 8, the dislocation density decreases with increasing In content, which can be ascribed to the improvement of the crystallinity leading to a decrease of donor sites trapped at the dislocations and grain boundaries.

The wavelength dependence of optical transmittance of In doped CdSe films are shown in figure 9. The transmittance increases with increasing In content up to In = 12 wt% and after this decreases for heavily doped CdSe film. Two onsets of absorption edge are observed for every sample and the absorption edge is blue-shifted. The blue-shift indicates that the films consist of nanoparticles $G < 20$ nm [33]. The charge carriers are localized in nanocrystals and this leads to a blue-shift in the band gap (effect of quantum confinement) [14].

The magnitude of absorption coefficient, α, for In doped CdSe films deposited at room temperature is of the order of 10^4 cm^{-1}. The values of the two distinct optical band gaps were determined with the help of absorption spectra and found to vary continuously with the dopant ratio, as shown in figure 10.

The temperature dependence of the electrical conductivity $\sigma(T)$ for as-deposited In doped CdSe films in the range of
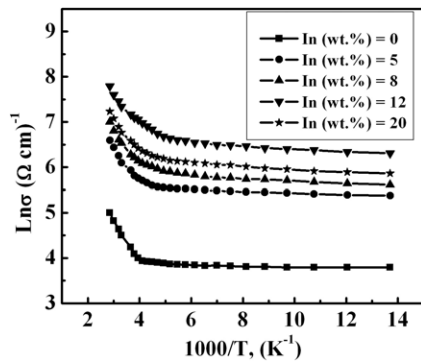
Figure 11. Ln σ versus $1000/T$ plots as a function of In content (wt%).
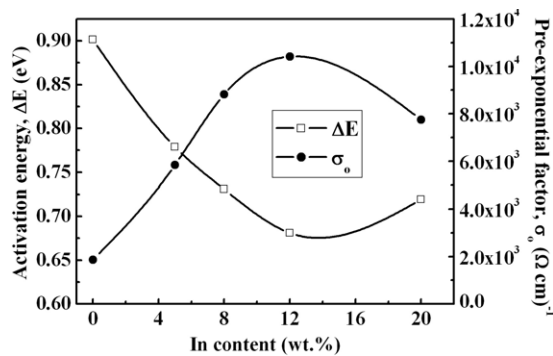

Figure 12. Variations of the activation energy and pre-exponential factor with In content (wt%).

T from 73 to about 350 K is shown in figure 11. The plot suggests that there are two types of conduction channels that contribute to the conductivity. While σ is nearly insensitive to temperature in the wide low range, it seems to be thermally activated in the high range of T and can be described by the relation

$$\sigma = \sigma_0 \exp(-\Delta E/KT) \tag{5}$$

where ΔE is the corresponding activation energy, representing the average energy of carriers with respect to the Fermi energy, and σ_0 is the pre-exponential factor. The activation energies in the corresponding high temperature regime were estimated and plotted in figure 12 as a function of In content. Figure 12 also shows the variation of the pre-exponential factor with In content. It is seen that the activation energy decreases from 0.9 to 0.68 eV on increasing the dopant ratio, whereas the electrical conductivity, σ_0, increases with increasing In content, which can be attributed to the increase in grain size and film crystallinity.

4. Conclusion

Thin films of $(CdSe)_{90}(In_2O_3)_{10}$, $(CdSe)_{90}(SnO_2)_{10}$ and $(CdSe)_{90}(ZnO)_{10}$ have been grown on glass substrates by the electron beam evaporation technique by mixing CdSe with In_2O_3, SnO_2 and ZnO powders respectively to form three different compounds. It has been found that undoped and Sn

or In doped CdSe films have two direct transitions due to spin–orbit splitting of the valence band. These splittings are also noticed in the transmittance spectra of CdSe thin films at 750 and 1250 nm for undoped film and at 750 and 1095 nm for Sn doped CdSe, 750 and 1300 nm for In doped CdSe. The electrical resistivity for n-doped CdSe thin films as a function of light exposure time has been studied. It has been found that the electrical resistivity decreases with increasing light exposure time and the In doped CdSe thin film has the lowest value of resistivity. The influence of doping on the structural, optical and electrical characteristics of In doped CdSe films has been investigated in detail. It was established that the film with In (wt%) = 12 has the highest transmittance of $\sim 78\%$ in the visible region at wavelength equal to 750 nm and over 88% in the NIR region at 1310 nm. The DC conductivity of the films was measured in vacuum by the two-probe technique. The activation energy decreased from 0.9 to 0.68 eV on increasing the dopant ratio, whereas the electrical conductivity, σ_0, increased with increasing In content.

References

[1] Padiyan D P, Marikani A and Murali K R 2005 *Physica* B **357** 485–93

[2] Benkakou A F, Aourag H and Certier M 2000 *Mater. Chem. Phys.* **66** 10

[3] Hankare P P, Bhuse V M, Garadkar K M, Delekar S D and Mulla I S 2003 *Mater. Chem. Phys.* **82** 711

[4] Pejova B, Tanuševski A and Grozdanov I 2003 *J. Solid State Chem.* **174** 276

[5] Moreno O P, Morales R L, Falfán M R, Álvareza J P, Angel O Z and López L B 2000 *J. Phys. Chem. Solids* **61** 1751

[6] Calster A V, Vervaet A, De Rycke I, De Baets J and Vanfleteren J 1988 *J. Cryst. Growth* **86** 924

[7] Lokhande C D, Lee E-H, Jung K-D and Joo O-S 2005 *Mater. Chem. Phys.* **91** 200–4

[8] Husain M, Singh B P, Kumar S, Sharma T P and Sebastian P J 2003 *Sol. Energy Mater. Sol. Cells* **76** 399

[9] Baban C and Rusu G I 2003 *Appl. Surf. Sci.* **211** 6

[10] Murali K R, Srinivasan K and Trivedi D C 2005 *Mater. Lett.* **59** 15

[11] SU B and Choy K L 2000 *J. Mater. Sci. Lett.* **19** 1859

[12] Perna G, Capozzi V, Minafra A, Pallara M and Ambrico M 2003 *Eur. Phys. J.* B **32** 339

[13] Bhattacharya C and Datta J 2005 *Mater. Chem. Phys.* **89** 170

[14] Němec P, Mikeš D, Rohovec J, Uhlířová E, Trojánek F and Malý P 2000 *Mater. Sci. Eng.* B **B69/70** 500

[15] Velumani S, Mathew X, Sebastian P J, Narayandassb Sa K and Mangalaraj D 2003 *Sol. Energy Mater. Sol. Cells* **76** 347

[16] Nikale V M and Bhosale C H 2004 *Sol. Energy Mater. Sol. Cells* **82** 3

[17] Kh Shokr E, Wakkad M M, Abd El-Ghanny H A and Ali H M 1999 *Eur. Phys. J. Appl. Phys.* **8** 215

[18] Kh Shokr E, Wakkad M M, Abd El-Ghanny H A and Ali H M 2000 *J. Phys. Chem. Solids* **61** 75

[19] Ali H M, Mohamed H A and Mohamed S H 2005 *Eur. Phys. J. Appl. Phys.* **31** 87

[20] Mohamed S H, Ali H M, Mohamed H A and Salem A M 2005 *Eur. Phys. J. Appl. Phys.* **31** 95

[21] Ali H M 2005 *Phys. Status Solidi* a **202** 2742

[22] Mohamed H A, Ali H M, Mohamed S H and Abd El-Raheem M M 2006 *Eur. Phys. J. Appl. Phys.* **34** 7

[23] Ali H M, Mohamed H A, Wakkad M M and Hasaneen M F 2007 *Thin Solid Films* **515** 3024

[24] Ali H M, Abd El-Raheem M M, Megahed N M and
 Mohamed H A 2006 *J. Phys. Chem. Solids* **67** 1823
[25] Tauc J, Grigorovici R and Vancu A 1966 *Phys. Status Solidi* a
 15 627
[26] Hankare P P, Jadhav A D, Bhuse V M, Khomane A S and
 Garadkar K M 2003 *Mater. Chem. Phys.* **80** 102–7
[27] Velumani S, Mathew X, Sebastiana P J, Narayandass Sa K
 and Mangalaraj D 2003 *Sol. Energy Mater. Sol. Cells*
 76 347

[28] Pejova B, Tanuševski A and Grozdanov I 2004 *J. Solid State
 Chem.* **177** 4785
[29] Tabet-Derraz H, Benramdane N, Nacer D, Bouzidi A and
 Medles M 2002 *Sol. Energy Mater. Sol. Cells* **73** 249
[30] Fallah H R, Ghasemi M, Hassanzadeh A and Steki H 2006
 Physica B **373** 274
[31] Chaure S, Chaure N B and Pandey R K 2005 *Physica* E **28** 439
[32] Williamson G and Smallman R 1956 *Phil. Mag.* **1** 34
[33] Kale R B and Lokhande C D 2004 *Appl. Surf. Sci.* **223** 343–51